Supporting Information

Mechanistic Study of Oxygen Reduction at Liquid/Liquid Interfaces by Hybrid Ultramicroelectrodes and Mass Spectrometry

Chaoyue Gu,[†] Xin Nie,[†] Jiezhang Jiang,[†] Zifei Chen,[†] Yifan Dong,[†] Xin Zhang,[†] Junjie Liu,[†] Zhengyou Yu,[†] Zhiwei Zhu,[†] Jian Liu,[†] Xiaoyun Liu,[‡] and Yuanhua Shao[*,†]

[†]*Beijing National Laboratory for Molecular Sciences, College of Chemistry and Molecular Engineering, Peking University, Beijing 100871, China*
[‡]*Department of Microbiology, School of Basic Medical Sciences, Peking University Health Science Center, Beijing 100191, China*

Corresponding Authors:
Prof. Yuanhua Shao, Email: yhshao@pku.edu.cn

Table of Contents

S1. Fabrication and Characterization of the Gel Hybrid Ultramicroelectrodes S-3

S2. Voltammetric Studies of Ion Transfer with the Gel Hybrid Ultramicroelectrodes S-6

S3. EC-MS Setup S-10

S4. Background Signal of Air Detected by MS S-11

S5. Biphasic Reactions S-11

S6. Homogeneous Oxygen Reduction Reaction S-13

S7. Theoretical Analysis S-14

S1. Fabrication and Characterization of the Gel Hybrid Ultramicroelectrodes

Characterization of the Agar-gel Ultramicroelectrodes. The radius of the agar-gel ultramicroelectrodes was obtained with the facilitated ion transfer of K^+ by DB18C6. The empty channel of the agar-gel ultramicroelectrodes was filled with aqueous solution and the pipette was put into DCE solution. The outer surface and bands of dual micropipette were silanized, avoiding the water phase diffuses to connect with the agar-gel microelectrode.[S1] The electrochemical cell S1 is as follows: Ag| AgCl | 100 mM KCl || 2 mM DB18C6 + 2 mM BTPPATPBCl | AgTPBCl| Ag. The radius can be calculated by the steady-state diffusion limiting current (i_{ss}): [S2]

$$i_{ss} = 4nFDCr \quad \text{(S1)}$$

where n is the transferred charge, F is the Faraday constant, D and C are the diffusion constant (5.2×10^{-6} cm^2/s) [S3] and the bulk concentration of DB18C6. The radius of dual-barrel micropipettes was about 710 nm obtained from the cyclic voltammetry, which was consistent with the ESEM image (about 700 nm shown in Figure 1a).

The influence of amount of agar (0.5-5%, w/w) was assessed as shown in Figure S1. The result showed the concentration of agar had negligible effect on the electrochemical performance, e.g. the potential window. The concentration of the agar was a consideration of gelation time. When the concentration of agar was less than 1%, rather long time to gel was needed. Additionally, the gelation was instant with 5% concentration, making the injection to the micropipettes difficult. Thus, agar (2%, w/w) was chosen in follow-up experiments.

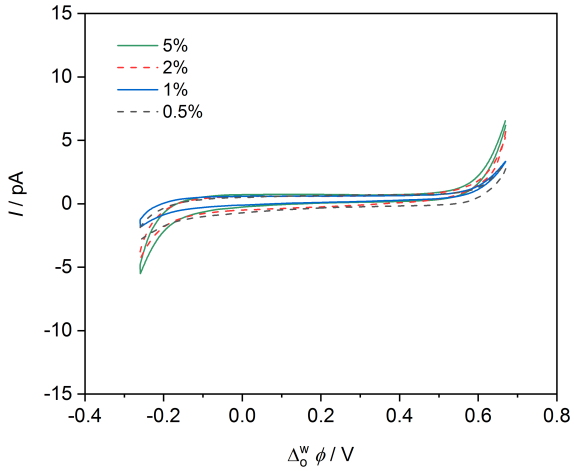

Figure S1. Effect of the concentration of agar (0.5-5%, w/w) on the electrochemical performance with cell S2: Ag| AgCl | x% agar + 10 mM LiCl || 5 mM BTPPATPBCl | AgTPBCl| Ag, scan rate: 0.02 V s^{-1}.

Fabrication of the PVC-gel Ultramicroelectrodes. The water/PVC-gel hybrid ultramicroelectrodes were fabricated based on dual micropipettes using the method which was similar to the previous report for single micropipette PVC-gel electrodes.[S4] The organogel was prepared by adding PVC in DCE solution (2-15%, m/v) and heated to about 80°C until the PVC dissolved. Using a small syringe, the hot organogel was backfilled into one channel of the dual micropipettes. When organogel was cooled down to room temperature (22 ± 2°C), an aqueous phase was put into another channel, which would cover the outer surface and have a nice contact with PVC-gel. Then, the water/PVC-gel hybrid ultramicroelectrodes were obtained. The influence of amount of PVC was determined as shown in Figure S2. The results showed the potential windows of different concentrations of PVC were similar. When the concentration was less than 5%, the time to gel was rather long. Moreover, injecting organogel to the micropipettes was difficult with 15% concentration, due to the instant gelation of the PVC solution. The concentration of PVC used in this work was 10% concentration, which was determined by the gelation time.

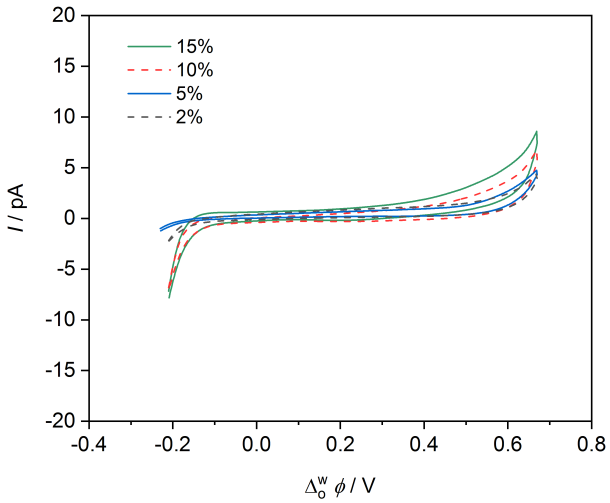

Figure S2. Effect of the concentration of PVC (2-15%, m/v) on the electrochemical performance with cell S3: Ag| AgCl | 10 mM LiCl || x% PVC + 5 mM BTPPATPBCl | AgTPBCl| Ag, scan rate: 0.02 V s^{-1}.

The optical microscopy image in Figure S3a shows that the gel filled into one tip of the dual barrels (below) and no air bubbles were inside the micropipette. Figure S3b is the ESEM image, which reveals that the gel at the tip was smooth.

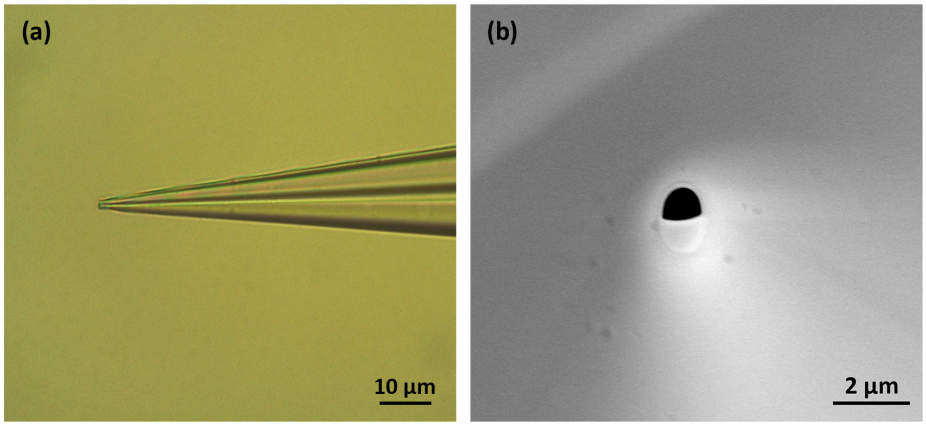

Figure S3. PVC-gel hybrid micropipettes recorded by optical microscopy (a) and ESEM (b).

Electrochemical Characterization of the Gel Hybrid Ultramicroelectrodes. The potential window of the agar-gel/DCE interface was tested using the electrochemical cell S4: Ag| AgCl | 2% agar + 10 mM LiCl || 5 mM BTPPATPBCl | AgTPBCl| Ag and the water/PVC-gel interface with cell S5: Ag| AgCl | 10 mM LiCl || 10% PVC + 5 mM BTPPATPBCl | AgTPBCl| Ag. The classical potential window at a water/DCE interface was also performed

without PVC or agar in the solution. Different from the water/PVC-gel and agar-gel/DCE interfaces that were based on the dual micropipette, the water/DCE interface was performed by putting pipette filled with water into external DCE. As shown in Figure S4, they had the similar potential windows, proving that the water/PVC-gel interface and agar-gel/DCE interface were very similar to that of a W/DCE interface and the PVC and agar were electrochemically inactive in the gel phases. Only the positive end and negative end of the gel microelectrode were larger about 80 mV, which would come from the larger resistance in the thin film formed in the dual micropipette than in the external solution or the impact of gel phase on the reference electrode.

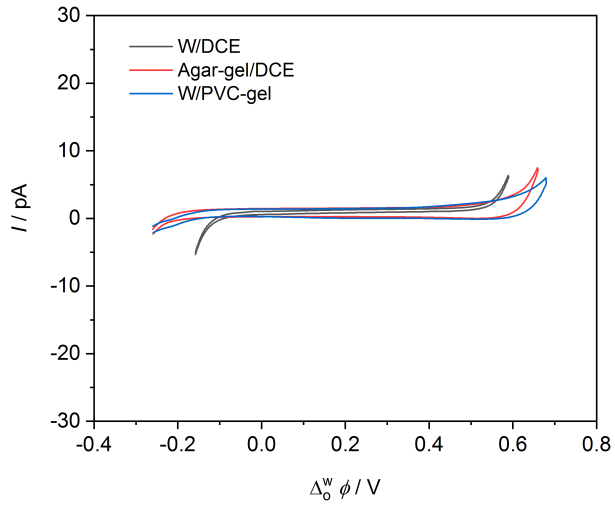

Figure S4. Potential windows of the agar-gel/DCE interface (red curve), water/PVC-gel interface (blue curve) and W/DCE interface (black curve), scan rate: 0.02 V s^{-1}.

S2. Voltammetric Studies of Ion Transfer with the Gel Hybrid Ultramicroelectrodes

The cells employed to examine the water/PVC-gel and agar-gel/organic hybrid ultramicroelectrodes are listed in the following:

Cell S6: Ag| AgCl | 10 mM LiCl || 10% PVC + 5 mM TEATPBCl + 5 mM BTPPATPBCl | AgTPBCl| Ag

Cell S7: Ag| AgCl | 2 mM TEACl + 10 mM LiCl || 10% PVC + 5 mM BTPPATPBCl | AgTPBCl| Ag

Cell S8: Ag| AgCl | 100 mM KCl || 10% PVC + 5 mM DB18C6 + 5 mM BTPPATPBCl | AgTPBCl| Ag

Cell S9: Ag| AgCl | 2% agar + 10 mM LiCl + 10 mM TMACl || 5 mM BTPPATPBF_5 | AgTPBF_5| Ag

Simple Ion Transfer of TEA^+ From Organogel to Aqueous Phase. Based on the PVC-gel hybrid ultramicroelectrodes with cell S6, the ion transfer of tetraethylammonium (TEA^+) from PVC-gel to aqueous phase was conducted and the voltammogram is shown in Figure S5a. Under a low sweep rate such as 0.01 V s^{-1}, the CV response showed an almost steady-state current resulting from sphere diffusion of TEA^+. With the increase of the sweep rate, the CV response changed into a peak curve. Clearly, the diffusion coefficient in the organic gel would be much smaller than that in the organic phase. To obtain the diffusion coefficient of the TEA^+ in the PVC-gel, the Randles-Sevcik equation was applied, which provides the relationship between the peak current and the sweep rate: [S5]

$$i_p = (2.69\times10^5)z^{3/2}AD^{1/2}Cv^{1/2} \quad \text{(S2)}$$

where i_p is the cathodic peak current, z is the charge number of the transferred ion, A is the area of the micro-L/L interface, D is the diffusion coefficient of the transferred species, C is the concentration of the transferred species and v is scan rate. The relationship between i_p and the square root of scan rates is shown in Figure S5b. From the equation S2, the diffusion coefficient of TEA^+ in the gel of organic solution was (5.5 ± 0.2) $\times10^{-7}$ cm^2 s^{-1}, which was consistent with the previous result.[S6]

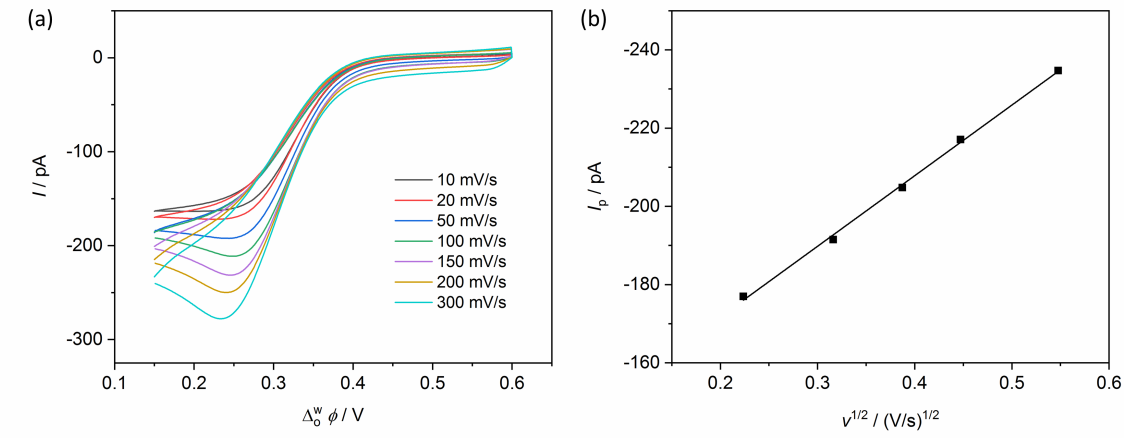

Figure S5. (a) Simple ion transfer of TEA^+ from organogel to aqueous phase by using cell S6. The radius of micropipette was about 3.4 μm; (b) The relationship between i_p and the square root of scan rates.

Simple Ion Transfer of TEA^+ From Aqueous Phase to Organogel. The simple ion transfer of TEA^+ from the aqueous phase to the organogel was also carried out with the electrochemical cell S7. As shown in Figure S6, a positive current due to the transfer of TEA^+ from water to PVC-gel was observed, showing that PVC-gel hybrid ultramicroelectrodes could be used to study the simple ion transfer and the interface was stable.

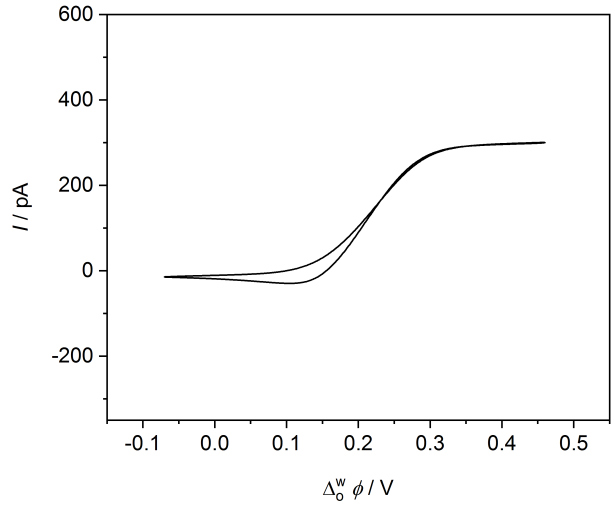

Figure S6. Simple ion transfer of TEA^+ from the aqueous phase to the organogel by using cell S7, scan rate: 0.05 V s^{-1}.

Facilitated Ion Transfer of DB18C6 From Organogel to Aqueous Phase. The facilitated ion transfer of K^+ by DB18C6 from the organogel to the aqueous phase was also performed using cell S8. As shown in Figure S7a, with the increase of the sweep rate, the steady-state current changed into a peak curve, which was corresponding to the diffusion pattern of the DB18C6 from sphere diffusion to linear diffusion. Using the same methodology, the diffusion coefficient of DB18C6 in the gel of organic solution was $(2.9 \pm 0.1) \times 10^{-7}$ cm^2 s^{-1} obtained from Figure S7b, which was consistent with the previous result.[S7]

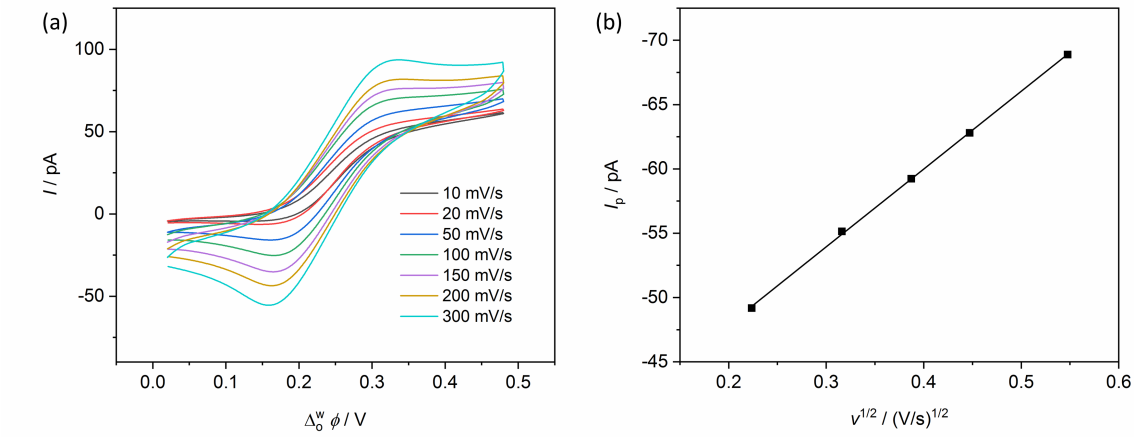

Figure S7. (a) Simple ion transfer of DB18C6 from the organogel to the aqueous phase by using cell S8. The radius of micropipette was about 2.3 μm; (b) The relationship between i_p and the square root of scan rates.

Simple Ion Transfer of TMA^+ From Agar-gel to Organic Phase. The simple ion transfer of TMA^+ at the agar-gel/organic interfaces was conducted with the electrochemical cell S9. A positive current resulted form the transfer of TMA^+ from agar-gel to organic phase was recorded (Figure S8), which was consistent with the EC-MS results.

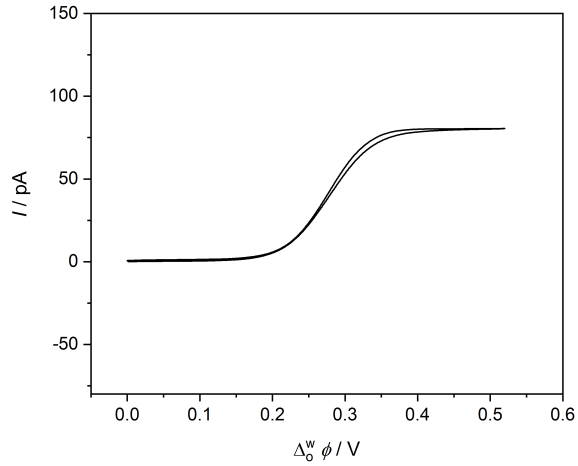

Figure S8. TMA^+ transfer from agar-gel to organic phase by using cell S9, scan rate: 0.05 V s^{-1}.

S3. EC-MS Setup

The experimental EC-MS setup is shown in Figure S9, including the hybrid gel ultramicroelectrode as the micro-EC cell, a MS as the detector, and a piezoelectric pistol as pulse ion source. By applying a proper potential to the micro-EC cell, the electrochemical reaction could take place at the L/L interface and the piezoelectric pistol (ca. 5 mm with the micro-EC cell) was used to induce the solution of the interfacial reaction spraying into the MS. The distance between the micro-EC cell and the MS inlet was quite short (ca. 2 mm), which enabled the determination of highly reactive intermediates generated at the surface of the electrodes.

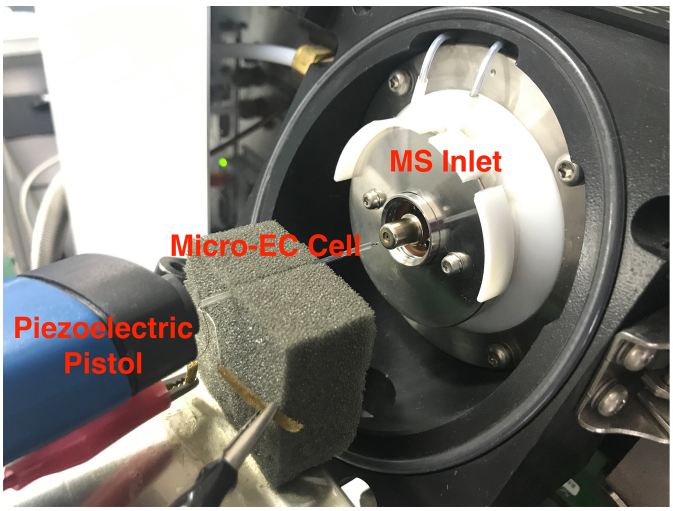

Figure S9. Photograph of the experimental EC-MS setup.

S4. Background Signal of Air Detected by MS

The agar-gel ultramicroelectrode with the other channel empty was induced by the piezoelectric pistol and the signal was recorded by the MS. As shown in Figure S10, the signal of TMA^+ in the agar gel was absent, revealing the successful immobilization of the aqueous phase by adding agar. The obtained signal should come from the ionization of volatile organic compounds in the air.

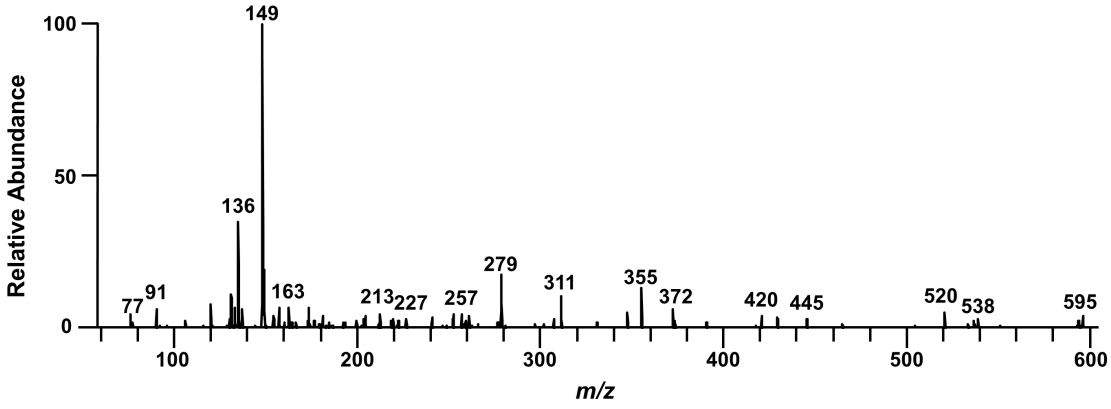

Figure S10. Background signals of air detected by MS.

S5. Biphasic Reactions

The ORR could proceed by a direct four-electron reduction to generate water or a two-electron reduction to produce hydrogen peroxide (H_2O_2). The biphasic reactions under chemically controlled polarization were performed to examine the final product of these reactions. The $TPBF_5^-$ was employed as the common ion by adding $LiTPBF_5$ and $BTPPATPBF_5$ in the same concentration of 5 mM to the macro-aqueous and macro-DCE phases, respectively. The interfacial Galvani potential difference was controlled at around 0.54 V,[S8] under which protons transferred from the aqueous to the organic phase, thus enabling the reduction of oxygen by Fc. For a fresh solution of 5 mM Fc and 50 μM CoTPP in 1.5 mL DCE (shown in Figure S11a, dotted line), the absorption bands at 439 nm (Fc) and 410 nm (CoTPP) were observed. The fresh solution was yellow, which would instantly turn to green at the interface of the two phases in contact with H_2SO_4 (pH=2.0), indicating the reaction took place at the interface (see inset). The aqueous and organic solutions were

separated after 1 h biphasic reaction and the UV-visible spectroscopic measurements were performed. As shown in the solid line of Figure S11a, this organic solution after 1h stirring showed a very large absorbance at 620 nm, which could be ascribed to Fc^+, indicating the oxidation of Fc to Fc^+. Besides, a Soret band shift from 410 nm to 427 nm was observed, consistent with proton facilitated oxygenation of CoTPP to form (Co-O_2)TPP. After treated with excess NaI (equivalent to 0.1 M), two absorption bands of aqueous phase at 286 and 352 nm (Figure S11b) were detected, which indicated the formation of H_2O_2 reduced by Fc with CoTPP as the molecular catalyst.

Time profiles of the formation of Fc^+ and H_2O_2 in the presence of CoTPP were carried out by biphasic reactions. As seen from Figure S11c, the generation of Fc^+ increased faster in a short time but turned slowly after 10 min, indicating that most of Fc were oxidized to Fc^+ before 10 min. Furthermore, the quantity of H_2O_2 also increased slowly after 10 min and decreased at longer time, e.g., after 60 min, as we can see in Figure S11d, which might attribute to the heterogeneous catalytic role of Fc towards the H_2O_2 decomposition. If assuming that the concentration of O_2 and proton was excess and Fc was completely oxidized after 120 min, the percentage of Fc used to produce H_2O_2 at 30 min was 5.7% in the biphasic reaction. The number of transferred electrons per molecular oxygen reduction was 3.9. As a result, CoTPP can catalyze the four-electron reduction of O_2, the selectivity of which was more than 94%, further confirming the high selectivity to produce H_2O. The biphasic reactions demonstrate this ORR mainly proceeds with a four-electron reduction pathway.

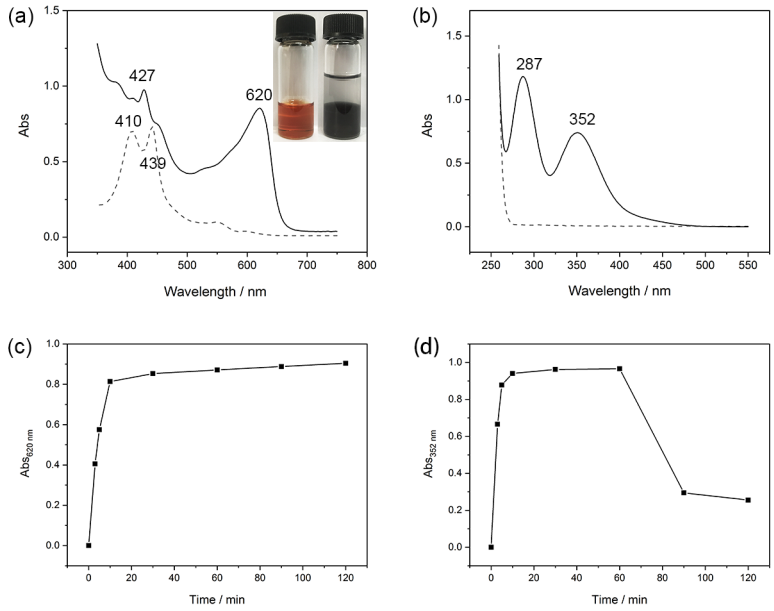

Figure S11. (a) UV−vis spectra of DCE phases containing 50 μM of CoTPP, 5 mM Fc, and 5 mM $BTPPATPBF_5$ before (dotted black) and after (full black) biphasic reactions, the inset shows the flasks before adding the aqueous solution (left) and after 1 h (right) biphasic reaction; (b) UV/Vis spectra of the water phase before (dotted black) and after (full black) treatment with 0.1m NaI after 1 h of the biphasic reaction; Time profile of the formation of Fc^+ (d) and H_2O_2 (d) in biphasic reaction.

S6. Homogeneous Oxygen Reduction Reaction

The homogeneous reaction was conducted to verify the two-electron oxygen reduction pathway. The different aspect from the heterogeneous oxygen reduction reaction was the direct addition of the acid in the DCE solution. Figure S12 (dotted black) shows the UV−vis spectra of DCE phase containing 50 μM of CoTPP, 5 mM Fc, and TFA (pH=2.0). After adding the excess TBAI in the reaction solution, the characteristic absorption peaks (292 nm and 364 nm) of I_3^- were detected (full red), the amount of which was determined from the absorption band at λ_{max}=364 nm (ε=25000 M^{-1} cm^{-1}).[S9] The absorption peak at 411 nm should be assigned to the CoTPP. Assuming that the concentration of proton and O_2 in the open experimental system was excess and Fc was completely oxidized in the homogeneous reaction, the percentage of Fc used to produce H_2O_2 was 72%. The number of transferred electrons per molecular oxygen reduction was 2.6, confirming the homogeneous reaction favours the two-electron oxygen reduction pathway.

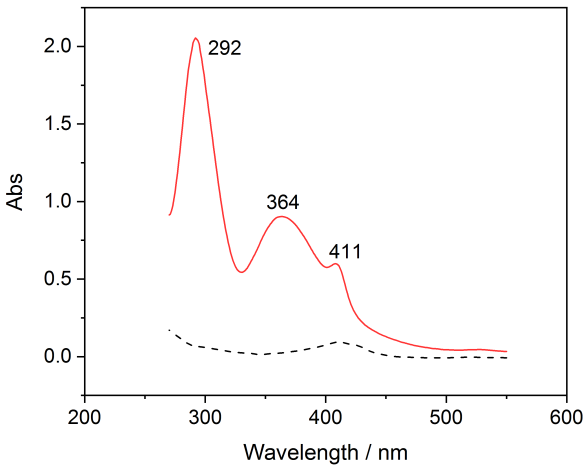

Figure S12. UV−vis spectra of DCE phase containing 50 μM of CoTPP, 5 mM Fc, and TFA (pH=2.0) before (dotted black) and after (full red) treated with TBAI (0.10 M). All the solutions were diluted for 50 times.

S7. Theoretical Analysis

Calculation was carried out to investigate the possibility of formation of the CoTPP intermediates in the four-electron oxygen reduction pathway. Density functional theory (DFT) within the Gaussian 09 program[S10] and the Becke-Lee-Yang-Parr exchange-correlation functional (BLYP) [S11, S12] were used in this work, which had been applied in similar systems before.[S13, S14] The correlation consistent polarized valence double zeta (cc-pVDZ) basis set[S15] was employed for all elements. The structures of intermediates (CoTPP, (Co-O_2)TPP, (Co-OOH)TPP, (Co=O)TPP, and (Co-OH)TPP, as shown in Figure S13) and other substances involved in the mechanism were fully optimized. We also applied the single-point polarizable continuum model (PCM) calculation with universal force field (UFF) atomic radii [S16] for all molecules to model the DCE and water solvent environment.[S17, S18]

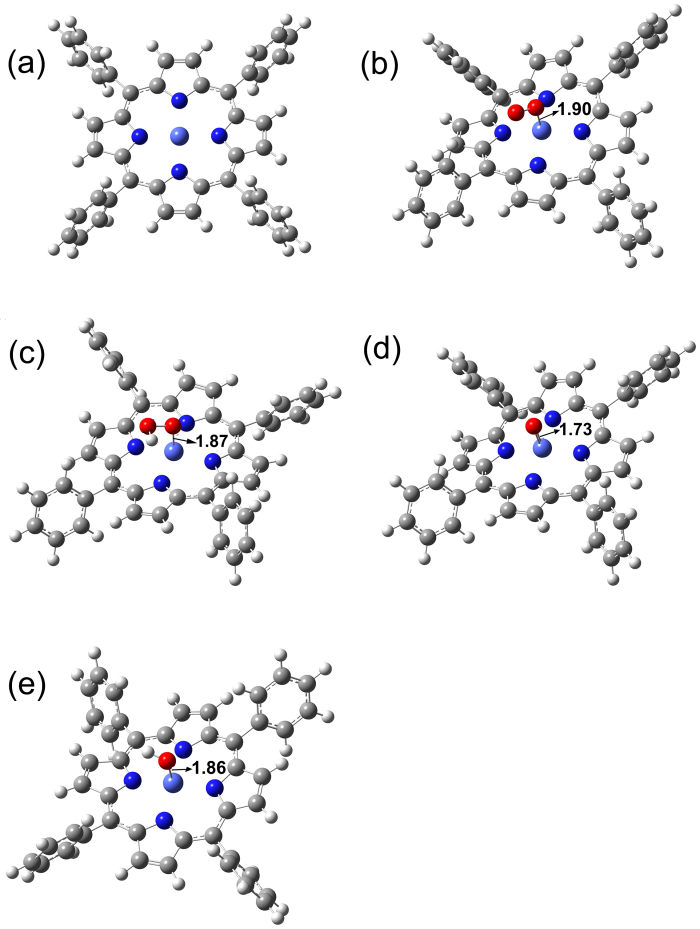

Figure S13. Optimized structures of (a) CoTPP, (b) (Co-O_2)TPP, (c) (Co-OOH)TPP, (d) (Co=O)TPP, and (e) (Co-OH)TPP. The selected Co-O bond length is presented in each structure.

The frequency analysis of the optimized structure was carried out at 298 K and 1 atm pressure, which were our experimental conditions, to obtain the Gibbs free energy (G). The final solvent-corrected free energy was obtained by adding the gas-phase free energy correction to the solvent electronic energy. Except that H_2O and proton are in water, DCE was the only solvent for all other structures in calculating the solvent effect corrections. The free energy of proton in water is obtained from a previous study (-262.4 Kcal/mol).[S19] All Gibbs free energies in our calculations are listed in Table S1, and free energy gaps in Figure 8 are also depicted in Table S2.

Table S1. The free energy of gas phase (G_{gas}) and solution (G_{sol}) and spin multiplicity ($2S+1$) of each molecule/ion based on the BLYP/cc-PVDZ level calculation at 298 K and 1 atm pressure.

	G_{gas} (Hartree)	G_{sol} (Hartree)	2*S*+1
O_2	-150.345598	-150.345764	3
CoTPP	-3294.389667	-3294.400521	2
(Co-O_2)TPP	-3444.747703	-3444.758171	2
(Co-OOH)TPP	-3445.332226	-3445.345663	1
(Co=O)TPP	-3369.549126	-3369.564620	2
(Co-OH)TPP	-3370.185601	-3370.199580	1
Fc	-1650.629488	-1650.632141	1
Fc^+	-1650.397074	-1650.460835	2
H_2O	-76.396248	-76.402098	1
H^+		-0.418161[S19]	1

The changes of Gibbs free energy for equations 5-9 (Figure 8g) are list below:

Eq 5: $Co^{II}TPP_{(DCE)} + O_{2(DCE)} \rightarrow (Co^{II}\text{-}O_2)TPP_{(DCE)}$

(-3444.758171 - (-150.345764 - 3294.400521)) × 27.2 = -0.323299 eV

Eq 6: $(Co^{II}\text{-}O_2)TPP_{(DCE)} + Fc_{(DCE)} + H^+_{(w)} \rightarrow (Co^{III}\text{-}OOH)TPP_{(DCE)} + Fc^+_{(DCE)}$

(-3445.345663 - 1650.460835 - (-3444.758171 - 1650.632141 - 0.418161)) × 27.2 = 0.053720 eV

Eq 7: $(Co^{III}\text{-}OOH)TPP_{(DCE)} + Fc_{(DCE)} + H^+_{(w)} \rightarrow (Co^{IV}\text{=}O)TPP_{(DCE)} + Fc^+_{(DCE)} + H_2O_{(w)}$

(-3369.564620 - 1650.460835 - 76.402098 - (-3445.345663 - 1650.632141 -0.418161)) × 27.2 = -0.8591936 eV

Eq 8: $(Co^{IV}\text{=}O)TPP_{(DCE)} + Fc_{(DCE)} + H^+_{(w)} \rightarrow (Co^{III}\text{-}OH)TPP_{(DCE)} + Fc^+_{(DCE)}$

(-3370.199580 - 1650.460835 - (-3369.564620 - 1650.632141 - 0.418161)) × 27.2 = -1.237410 eV

Eq 9: $(Co^{III}\text{-}OH)TPP_{(DCE)} + Fc_{(DCE)} + H^+_{(w)} \rightarrow Co^{II}TPP_{(DCE)} + Fc^+_{(DCE)} + H_2O_{(w)}$

(-3294.400521 - 1650.460835 - 76.402098 - (-3370.199580 - 1650.632141 -0.418161)) × 27.2 = -0.3691584 eV

The total Gibbs energy difference of Eqs 5-9 is:

-0.323299 + 0.053720 - 0.8591936 - 1.237410 - 0.3691584 = -2.735341 eV.

The total outcome of Eqs 5-9 is:

$O_{2(DCE)} + 4(Fc_{(DCE)} + H^{+}_{(w)}) = 4Fc^{+}_{(DCE)} + 2H_2O_{(w)}$

The change of Gibbs free energy is consistent with the sum of all ΔGs of equations 5-9:

(- 4 × 1650.460835 - 2 × 76.402098 - (-150.345764 - 4 × 1650.632141- 4 × 0.418161)) × 27.2 = -2.7353408 eV

Table S2. HOMO and LUMO energy gap (E_g) in Figure 8.

	CoTPP	(Co-O_2)TPP	(Co-OH)TPP
E_g (Hartree)	0.031010	0.007740	0.030680

The Cartesian coordinates of all optimized geometries are listed below (in Å):

O_2

O	-1.46479430	-0.39411764	-0.02962938
O	-2.69953114	-0.39411764	-0.01899975

CoTPP

C	-2.86527000	-1.08255000	0.00030000
C	-4.24900000	-0.64535000	0.00025000
C	-4.23612000	0.72517000	-0.00015000
C	-2.84440000	1.13619000	-0.00026000
N	-2.00051000	0.01883000	0.00001000
H	-5.11200000	-1.31522000	0.00046000
H	-5.08630000	1.41123000	-0.00032000
C	-2.43394000	2.48017000	-0.00049000
C	-0.64535000	4.24898000	-0.00024000
C	1.13620000	2.84438000	0.00027000
C	0.72518000	4.23609000	0.00015000
H	-1.31523000	5.11197000	-0.00045000
H	1.41127000	5.08626000	0.00030000
C	-1.08253000	2.86524000	-0.00030000
N	0.01882000	2.00049000	0.00000000
C	2.48018000	2.43394000	0.00050000
C	4.24901000	0.64533000	0.00027000
C	2.84441000	-1.13622000	-0.00027000

C	4.23612000	-0.72519000	-0.00012000
H	5.11202000	1.31519000	0.00050000
H	5.08629000	-1.41126000	-0.00027000
C	2.86526000	1.08252000	0.00030000
N	2.00052000	-0.01881000	0.00000000
C	2.43394000	-2.48019000	-0.00049000
C	0.64534000	-4.24901000	-0.00027000
C	-1.13621000	-2.84442000	0.00027000
C	-0.72518000	-4.23613000	0.00013000
H	1.31518000	-5.11204000	-0.00050000
H	-1.41122000	-5.08633000	0.00027000
N	-0.01882000	-2.00053000	0.00001000
C	1.08254000	-2.86528000	-0.00030000
C	-2.48018000	-2.43395000	0.00049000
Co	0.00000000	-0.00001000	0.00001000
C	3.49241000	-3.55842000	-0.00085000
C	3.99812000	-4.07281000	-1.21810000
C	3.99801000	-4.07375000	1.21605000
C	4.98469000	-5.07751000	-1.21844000
H	3.61226000	-3.67933000	-2.16917000
C	4.98458000	-5.07844000	1.21572000
H	3.61205000	-3.68100000	2.16739000
C	5.48068000	-5.58311000	-0.00153000
H	5.36660000	-5.46590000	-2.17374000
H	5.36641000	-5.46756000	2.17076000
H	6.25115000	-6.36749000	-0.00180000
C	-3.55843000	-3.49239000	0.00084000
C	-4.07376000	-3.99798000	-1.21607000
C	-4.07286000	-3.99808000	1.21808000
C	-5.07847000	-4.98454000	-1.21574000
H	-3.68099000	-3.61203000	-2.16741000
C	-5.07757000	-4.98464000	1.21841000
H	-3.67940000	-3.61220000	2.16915000
C	-5.58316000	-5.48063000	0.00150000
H	-5.46758000	-5.36636000	-2.17079000
H	-5.46599000	-5.36653000	2.17371000
H	-6.36754000	-6.25108000	0.00176000
C	-3.49238000	3.55842000	-0.00084000
C	-3.99779000	4.07312000	-1.21809000
C	-3.99826000	4.07347000	1.21606000
C	-4.98436000	5.07782000	-1.21843000
H	-3.61169000	3.67987000	-2.16916000

C	-4.98483000	5.07817000	1.21572000
H	-3.61253000	3.68050000	2.16740000
C	-5.48064000	5.58313000	-0.00152000
H	-5.36603000	5.46645000	-2.17373000
H	-5.36688000	5.46708000	2.17076000
H	-6.25110000	6.36751000	-0.00179000
C	3.55841000	3.49240000	0.00085000
C	4.07376000	3.99798000	-1.21605000
C	4.07278000	3.99814000	1.21810000
C	5.07845000	4.98455000	-1.21571000
H	3.68103000	3.61201000	-2.16739000
C	5.07747000	4.98471000	1.21844000
H	3.67929000	3.61229000	2.16917000
C	5.58310000	5.48067000	0.00154000
H	5.46759000	5.36636000	-2.17075000
H	5.46585000	5.36664000	2.17375000
H	6.36747000	6.25114000	0.00180000

(Co-O_2)TPP

C	2.51552600	1.66220800	0.00322300
C	3.95152000	1.57234900	-0.18874000
C	4.23325100	0.26605800	-0.50042000
C	2.97952000	-0.46456100	-0.44013900
N	1.92390400	0.41254200	-0.17471400
H	4.64184700	2.41710200	-0.13017000
H	5.20349900	-0.17675700	-0.73596100
C	2.87549600	-1.86584500	-0.52907100
C	1.57360800	-3.98790600	-0.12144600
C	-0.45614000	-3.01587100	0.17401000
C	0.27061400	-4.27194100	0.20207700
H	2.41320600	-4.68114000	-0.21052900
H	-0.17216700	-5.24594200	0.42150400
C	1.66584800	-2.54961200	-0.29375100
N	0.41354700	-1.95879100	-0.11099700
C	-1.85391600	-2.90506100	0.30630000
C	-3.97641200	-1.60963200	-0.11742500
C	-3.00806900	0.42495800	-0.40053300
C	-4.26139100	-0.30701800	-0.44076700
H	-4.66577800	-2.45421800	-0.04691400
H	-5.23317200	0.13108000	-0.67860300
C	-2.53937500	-1.69660700	0.06706100
N	-1.94888000	-0.44680600	-0.12831900

C	-2.90539100	1.82382300	-0.52986800
C	-1.59623100	3.95452700	-0.19358200
C	0.43410500	2.98537000	0.10323300
C	-0.29057400	4.24275600	0.11510800
H	-2.43652500	4.64658200	-0.28489900
H	0.15525700	5.21954200	0.31520400
N	-0.43729000	1.92610600	-0.15937500
C	-1.69149100	2.51282700	-0.33741600
C	1.83129800	2.87235800	0.23755200
Co	-0.00767300	-0.00933700	0.02675000
C	-4.14828100	2.62809400	-0.81454200
C	-4.32190600	3.24803500	-2.07559200
C	-5.15905600	2.78933100	0.16406700
C	-5.47726000	4.00265500	-2.35291100
H	-3.54477100	3.12875800	-2.84356900
C	-6.31255100	3.54696000	-0.11272800
H	-5.03007800	2.32342700	1.15092900
C	-6.47623100	4.15464100	-1.37245400
H	-5.59718700	4.47170200	-3.34022600
H	-7.08419100	3.66593600	0.66161000
H	-7.37789400	4.74548500	-1.58844800
C	2.64343800	4.09799200	0.56756800
C	2.85139500	5.12777100	-0.38150100
C	3.22549500	4.22925200	1.85154900
C	3.62025900	6.26052700	-0.05352600
H	2.41420200	5.03138100	-1.38523500
C	3.99063200	5.36417200	2.17920300
H	3.06484500	3.43588100	2.59458700
C	4.19085300	6.38288400	1.22800300
H	3.77664800	7.04837700	-0.80459400
H	4.43017800	5.45261800	3.18324200
H	4.79015100	7.26847400	1.48373200
C	4.11388900	-2.67706200	-0.81523300
C	4.27491000	-3.31087600	-2.07090900
C	5.13268700	-2.82965700	0.15622200
C	5.42617000	-4.07107600	-2.35015100
H	3.49127600	-3.19814700	-2.83327300
C	6.28214900	-3.59285800	-0.12246400
H	5.01373000	-2.35187700	1.13866800
C	6.43338700	-4.21457100	-1.37686400
H	5.53640200	-4.55112800	-3.33329700
H	7.06059600	-3.70467000	0.64610500

H	7.33192900	-4.80960300	-1.59437800
C	-2.66467600	-4.13434200	0.62868500
C	-2.84944300	-5.16625900	-0.32331300
C	-3.27013900	-4.27031700	1.90128300
C	-3.61601400	-6.30430700	-0.00924100
H	-2.39523100	-5.06680600	-1.31909900
C	-4.03327600	-5.41041500	2.21577900
H	-3.13208700	-3.47625100	2.64838600
C	-4.20887100	-6.43085800	1.26173700
H	-3.75338900	-7.09303700	-0.76308300
H	-4.49066400	-5.50133200	3.21158400
H	-4.80644600	-7.32055900	1.50689500
O	0.59339000	0.89615400	2.57072100
O	-0.02490400	-0.02259000	1.92840200

(Co-OOH)TPP

C	-2.98747000	-0.34098800	-0.40974400
C	-4.21284600	0.42571800	-0.55186300
C	-3.88555200	1.74235200	-0.35567500
C	-2.45266100	1.79321000	-0.12777400
N	-1.89983000	0.51432700	-0.20451800
H	-5.19447100	-0.00068200	-0.76990500
H	-4.54268900	2.61451000	-0.38474800
C	-1.74287800	2.98751900	0.10096200
C	0.42801200	4.26811400	0.21980200
C	1.79760500	2.49900800	-0.16143800
C	1.74580200	3.93618700	0.03696800
H	0.00051400	5.25578700	0.40601100
H	2.61667700	4.59545700	0.04931000
C	-0.33764700	3.04075400	0.09911300
N	0.51353100	1.95240700	-0.11315700
C	2.99336100	1.78074200	-0.35039000
C	4.26641000	-0.39130500	-0.49620100
C	2.50175400	-1.76201800	-0.09986000
C	3.93685600	-1.70937200	-0.31172500
H	5.25046100	0.03659200	-0.70008100
H	4.59474000	-2.58095400	-0.34095200
C	3.03994100	0.37446000	-0.36391400
N	1.94954100	-0.48062400	-0.17423800
C	1.79073200	-2.95931600	0.10956600
C	-0.38482700	-4.24131800	0.19991300
C	-1.75130100	-2.47026400	-0.19217700

C	-1.70192500	-3.90672800	0.00374400
H	0.03834800	-5.23109300	0.38535700
H	-2.57244000	-4.56674500	0.00238000
N	-0.46654700	-1.92475300	-0.12319300
C	0.38421100	-3.01555800	0.09135600
C	-2.94298700	-1.74685700	-0.39572800
Co	0.01822800	0.01566300	0.01858500
C	2.57160000	-4.23377500	0.30518100
C	2.60965200	-5.23086600	-0.69972100
C	3.29117100	-4.45459100	1.50462100
C	3.34425900	-6.41633300	-0.50903000
H	2.06486100	-5.06660000	-1.63988500
C	4.02131600	-5.64250100	1.69690400
H	3.26934100	-3.68785900	2.29168800
C	4.05044500	-6.62710300	0.69085200
H	3.36698400	-7.17635700	-1.30340100
H	4.56863500	-5.79875900	2.63774100
H	4.62266900	-7.55389500	0.84033800
C	-4.22803800	-2.51782900	-0.56329600
C	-4.48117200	-3.24080800	-1.75405500
C	-5.20363700	-2.54012200	0.46274900
C	-5.67961300	-3.96106900	-1.91673700
H	-3.73254300	-3.22883400	-2.55862000
C	-6.39943700	-3.26504100	0.30165100
H	-5.01504600	-1.98861500	1.39437900
C	-6.64213500	-3.97619700	-0.88923000
H	-5.86169000	-4.51103400	-2.85138600
H	-7.14307500	-3.27524200	1.11162600
H	-7.57715900	-4.54054800	-1.01569200
C	-2.52570900	4.25954900	0.30421300
C	-2.57540000	5.25820800	-0.69823700
C	-3.23474400	4.47418900	1.51082200
C	-3.31264600	6.44065000	-0.49849000
H	-2.03713200	5.09829500	-1.64296900
C	-3.96740500	5.65913100	1.71169900
H	-3.20029900	3.70635600	2.29619800
C	-4.00919300	6.64573300	0.70797400
H	-3.34447300	7.20280000	-1.29053800
H	-4.50628400	5.81180400	2.65799000
H	-4.58330100	7.57020300	0.86469700
C	4.27948600	2.55308400	-0.50186000
C	4.54960300	3.27042500	-1.69224300

C	5.23927700	2.58187500	0.53874900
C	5.74939700	3.99159200	-1.84041500
H	3.81298900	3.25378400	-2.50775900
C	6.43646800	3.30752700	0.39201400
H	5.03634100	2.03670800	1.47106400
C	6.69631100	4.01298900	-0.79864300
H	5.94459400	4.53759400	-2.77475000
H	7.16736500	3.32348700	1.21341500
H	7.63228300	4.57824000	-0.91363100
O	0.11181800	0.04963400	1.89051600
O	-1.04242000	-0.51428500	2.53674700
H	-0.78707500	-1.46792800	2.59552600

(Co=O)TPP

C	-2.69033200	-1.42026800	-0.11302200
C	-4.09420500	-1.16904500	-0.37345300
C	-4.23547300	0.18472800	-0.54903000
C	-2.92427000	0.77632600	-0.36450000
N	-1.96788100	-0.22550800	-0.16700800
H	-4.86408100	-1.94180600	-0.43175200
H	-5.14548100	0.74470700	-0.77531700
C	-2.69315500	2.16292500	-0.29425900
C	-1.16789800	4.11496900	0.18856600
C	0.77557900	2.94400000	0.19348800
C	0.18487500	4.25894500	0.36422000
H	-1.94038700	4.88617900	0.23038800
H	0.74469700	5.17301000	0.57421000
C	-1.41624200	2.70591100	-0.05828500
N	-0.21921400	1.99094300	-0.03287300
C	2.15955600	2.69950500	0.14718700
C	4.09405800	1.16939200	-0.37292900
C	2.92406100	-0.77582100	-0.36530200
C	4.23522900	-0.18421100	-0.54985400
H	4.86391400	1.94219200	-0.43105900
H	5.14521500	-0.74407200	-0.77649700
C	2.69024900	1.42063700	-0.11212600
N	1.96771400	0.22605200	-0.16682200
C	2.69278400	-2.16217000	-0.29486400
C	1.16799600	-4.11367200	0.19156500
C	-0.77526900	-2.94262400	0.19421000
C	-0.18464400	-4.25752400	0.36727900
H	1.94070400	-4.88457600	0.23493800

H	-0.74445800	-5.17122200	0.57888000
N	0.21910700	-1.98977500	-0.03371700
C	1.41584400	-2.70472500	-0.05765500
C	-2.15935700	-2.69876200	0.14658600
Co	-0.00010300	0.00202200	0.12369700
C	3.86013600	-3.10508200	-0.43748300
C	3.98686600	-3.91975100	-1.58879500
C	4.84599500	-3.20364900	0.57424300
C	5.07292300	-4.80423900	-1.72728000
H	3.22936400	-3.85023200	-2.38203500
C	5.92858800	-4.09269900	0.43747300
H	4.75211300	-2.58428700	1.47701500
C	6.04688000	-4.89398800	-0.71443800
H	5.15815100	-5.42432300	-2.63136200
H	6.68082700	-4.16085500	1.23658400
H	6.89393300	-5.58661900	-0.82160100
C	-3.11623400	-3.84746700	0.33540100
C	-3.25025800	-4.85840700	-0.64709100
C	-3.91030400	-3.92936500	1.50512600
C	-4.15430300	-5.92178300	-0.46463800
H	-2.64689500	-4.80047400	-1.56380400
C	-4.80960500	-4.99621300	1.68911300
H	-3.81083500	-3.15300200	2.27643000
C	-4.93522500	-5.99517800	0.70476500
H	-4.24998500	-6.69423300	-1.24140300
H	-5.41278200	-5.04704900	2.60706600
H	-5.63939100	-6.82730600	0.84780300
C	-3.86082600	3.10551600	-0.43659100
C	-3.98887800	3.91916600	-1.58848000
C	-4.84581700	3.20465900	0.57592400
C	-5.07529100	4.80326500	-1.72671000
H	-3.23211600	3.84914900	-2.38238700
C	-5.92880800	4.09326000	0.43938800
H	-4.75101400	2.58601100	1.47909400
C	-6.04836400	4.89357600	-0.71307200
H	-5.16151400	5.42256600	-2.63123500
H	-6.68037300	4.16182400	1.23909800
H	-6.89571800	5.58586500	-0.82005400
C	3.11677200	3.84792100	0.33612000
C	3.25204100	4.85830100	-0.64679200
C	3.91005100	3.93006700	1.50636800
C	4.15640200	5.92138700	-0.46419300

H	2.64940900	4.80014700	-1.56397600
C	4.80973200	4.99657400	1.69047400
H	3.80972700	3.15410500	2.27797100
C	4.93649900	5.99501700	0.70574100
H	4.25301100	6.69339800	-1.24128200
H	5.41230100	5.04756300	2.60881800
H	5.64093500	6.82689800	0.84888100
O	0.00191200	-0.01582100	1.85566700

(Co-OH)TPP

C	3.03190000	0.15012100	-0.34300900
C	4.20258700	-0.70119000	-0.45386900
C	3.78415100	-1.98719200	-0.22654300
C	2.34863200	-1.93638800	-0.01734500
N	1.88539000	-0.62414500	-0.12967300
H	5.21336400	-0.34843800	-0.67018000
H	4.38147700	-2.90180000	-0.22670900
C	1.55394200	-3.07742600	0.20649800
C	-0.69965400	-4.21320600	0.25209900
C	-1.93614600	-2.35711000	-0.16755700
C	-1.98562100	-3.79518800	0.02478300
H	-0.34599400	-5.22676900	0.45294700
H	-2.89809300	-4.39541700	0.00847300
C	0.14912900	-3.03929300	0.15748200
N	-0.62081600	-1.89771700	-0.08266700
C	-3.07742800	-1.55760200	-0.36692900
C	-4.20299000	0.69770600	-0.45302900
C	-2.35100500	1.93477200	-0.01991700
C	-3.78724900	1.98415100	-0.22561400
H	-5.21347900	0.34306300	-0.66753900
H	-4.38624300	2.89764200	-0.22303300
C	-3.03004100	-0.15191700	-0.34604800
N	-1.88486900	0.62297200	-0.13660600
C	-1.55873400	3.07407800	0.21525400
C	0.69574300	4.20677200	0.27870000
C	1.93891100	2.35305100	-0.13861100
C	1.98396300	3.78905300	0.05466600
H	0.34091900	5.22128400	0.47305800
H	2.89492400	4.39159500	0.03614800
N	0.62089800	1.88891800	-0.04553900
C	-0.15258300	3.03483000	0.18527900
C	3.07933400	1.55570100	-0.35503100

Co	0.00056800	-0.00304700	0.06124300
C	-2.25074300	4.39337800	0.44850200
C	-2.26086000	5.40213800	-0.54500400
C	-2.91579900	4.64188200	1.67343100
C	-2.91755800	6.62656200	-0.31881000
H	-1.75664100	5.21730900	-1.50389200
C	-3.56820400	5.86828600	1.90055100
H	-2.91326600	3.86615900	2.45189300
C	-3.57173100	6.86413100	0.90525600
H	-2.92028300	7.39606000	-1.10433800
H	-4.07467600	6.04566900	2.86031200
H	-4.08331500	7.82108300	1.08213600
C	4.40673000	2.24244100	-0.55605200
C	4.68376100	2.92105700	-1.76742900
C	5.39677300	2.23262700	0.45618500
C	5.91858200	3.56766100	-1.96317700
H	3.92388800	2.93362600	-2.56139800
C	6.62973200	2.88335400	0.26155000
H	5.19095400	1.71595200	1.40404000
C	6.89519000	3.55152000	-0.94911800
H	6.11790300	4.08451500	-2.91304900
H	7.38437100	2.86997500	1.06122500
H	7.85887600	4.05838400	-1.10122600
C	2.24673100	-4.39426700	0.44743900
C	2.25825000	-5.40987100	-0.53921300
C	2.91294400	-4.63315600	1.67380700
C	2.91708900	-6.63157000	-0.30489700
H	1.75402600	-5.23234700	-1.49944900
C	3.56696500	-5.85702900	1.90908600
H	2.90679700	-3.85275600	2.44740100
C	3.57190000	-6.85971900	0.92061300
H	2.92084600	-7.40639500	-1.08517500
H	4.07297700	-6.02755500	2.87034700
H	4.08493900	-7.81469900	1.10392500
C	-4.40796400	-2.24146200	-0.55598800
C	-4.70133900	-2.91383600	-1.76682600
C	-5.38434300	-2.23535500	0.46954200
C	-5.93953100	-3.55796100	-1.94964200
H	-3.95178900	-2.92379500	-2.57062600
C	-6.62047100	-2.88364400	0.28759900
H	-5.16381700	-1.72543300	1.41764300
C	-6.90277300	-3.54539700	-0.92286800

H	-6.15178700	-4.07027600	-2.89919200
H	-7.36427600	-2.87399500	1.09743100
H	-7.86899800	-4.05042700	-1.06480900
O	-0.01760100	-0.07144600	1.92222300
H	0.46660900	0.73846600	2.19890800

Fc

C	-1.68731400	-0.99092000	-0.72426000
H	-1.67708500	-1.87460300	-1.37123000
C	-1.68829900	-0.99523600	0.71812800
H	-1.67832500	-1.88353600	1.35872300
C	-1.68942700	0.37547400	1.16798400
H	-1.68329700	0.71095500	2.21057400
C	-1.68798700	0.38247600	-1.16581200
H	-1.67985900	0.72469400	-2.20628700
C	-1.68909000	1.22673500	0.00352600
H	-1.68148200	2.32196200	0.00746100
C	1.68809500	-0.32962800	-1.18176400
H	1.68113000	-0.62440000	-2.23657400
C	1.68813400	-1.22578300	-0.05135800
H	1.67860900	-2.32004900	-0.09762100
C	1.68883400	-0.42774500	1.15014700
H	1.68136900	-0.80985100	2.17659800
C	1.68833100	1.02238400	-0.67878800
H	1.67902500	1.93487400	-1.28442100
C	1.68857400	0.96161900	0.76232600
H	1.68116400	1.81927800	1.44350500
Fe	-0.00001400	0.00017000	-0.00005800

Fc^+

C	-1.69874500	-0.79517300	-0.96549300
H	-1.66256300	-1.50713800	-1.79687100
C	-1.78092100	-1.12973800	0.43451800
H	-1.78792200	-2.14045000	0.85701600
C	-1.83284100	0.09392000	1.18279300
H	-1.86824300	0.17707300	2.27482200
C	-1.69750100	0.64599100	-1.07533400
H	-1.65986200	1.22407300	-2.00484500
C	-1.77906500	1.18914900	0.25729100
H	-1.78327600	2.25228500	0.52168400
C	1.83224700	-0.04326300	-1.18574900
H	1.86770700	-0.08098900	-2.28029400
C	1.77007800	-1.17632200	-0.30617800

H	1.77142300	-2.22763400	-0.61406500
C	1.69308200	-0.68716000	1.04863300
H	1.65478000	-1.30169900	1.95438000
C	1.78942300	1.14784800	-0.38740800
H	1.79932100	2.17512300	-0.76796500
C	1.70413600	0.75714600	0.99667200
H	1.66968500	1.43543100	1.85592300
Fe	-0.00001500	-0.00078700	0.00006700

H_2O

O	0.00000000	0.00000000	0.12349000
H	0.00000000	0.76045000	-0.49395000
H	0.00000000	-0.76045000	-0.49395000

Acknowledgement

ZC and JL thank Xinzheng Yang for useful discussions on the details of the calculation.

References

(S1) Liu, B.; Shao, Y.; Mirkin, M. V. *Anal. Chem*. **2000**, 72, 510-519.
(S2) Hu, H.; Xie, S.; Meng, X.; Jing, P.; Zhang, M.; Shen, L.; Zhu, Z.; Li, M.; Zhuang, Q.; Shao, Y. *Anal. Chem*. **2006**, 78, 7034-7039.
(S3) Shao, Y.; Mirkin, M. V. *J. Am. Chem. Soc.* **1997**, 119, 8103-8104.
(S4) Lee, H. J.; Beattie, P. D.; Seddon, B. J.; Osborne, M. D.; Girault, H. H. *J. Electroanal. Chem*. **1997**, 440, 73-82.
(S5) Li, F.; Chen, Y.; Zhang, M.; Jing, P.; Gao, Z.; Shao, Y. *J. Electroanal. Chem*. **2005**, 579, 89-102.
(S6) Liljeroth, P.; Johans, C.; Kontturi, K.; Manzanares, J. A. *J. Electroanal. Chem*. **2000**, 483, 37-46.
(S7) Lee, H. J.; Beriet, C.; Girault, H. H. *J. Electroanal. Chem*. **1998**, 453, 211-219.
(S8) Hatay, I.; Su, B.; Li, F.; Mendez, M. A.; Khoury, T.; Gros, C. P.; Barbe, J. M.; Ersoz, M.; Samec, Z.; Girault, H. H. *J. Am. Chem. Soc.* **2009**, 131, 13453-13459.
(S9) Fukuzumi, S.; Kotani, H.; Lucas, H. R.; Doi, K.; Suenobu, T.; Peterson, R. L.; Karlin, K. D. *J. Am. Chem. Soc.* **2010,** 132, 6874-6875.
(S10) Frisch, M.; et al. Gaussian 09, revision A. 01; Gaussian, Inc., Wallingford, CT. 2009.
(S11) Becke, A. D. *Phys. Rev. A* **1988**, 38, 3098–3100.
(S12) Lee, C. T.; Yang, W. T.; Parr, R. G. *Phys. Rev. B* **1988**, 37, 785–789.
(S13) Shi, Z.; Zhang, J. *J Phys Chem C* **2007,** 111, 7084-7090.
(S14) Sun, S.; Jiang, N.; Xia, D. *J Phys Chem C* **2011,** 115, 9511-9517.
(S15) Dunning, T. H. *J. Chem. Phys.* **1989,** 90, 1007-1023.

(S16) Rappe, A. K.; Casewit, C. J.; Colwell, K. S.; Goddard, W. A.; Skiff, W. M. *J. Am. Chem. Soc*. **1992**, 114, 10024.
(S17) Miertus, S.; Scrocco, E.; Tomasi, J. *Chem. Phys*. **1981,** 55, 117-129.
(S18) Cammi, R.; Tomasi, J. *J. Comput. Chem*. **1995,** 16, 1449-1458.
(S19) Zhang, C.; Dixon, D. *J. Phys. Chem. A* **2001**, 105, 11534-11540.